Dielectric coatings for elementary charge fluctuation studies testing with Kelvin probe microscopy

© V.D. Rodin[1,2], V.Yu. Aksenov[1], A.V. Ankudinov[1], V.O. Bolshakov[1], A.S. Vlasov[1], Yu.A. Zharova[1], I.V. Ulkiv[3], R.V. Levin[1], A.V. Malevskaya[1], A.M. Mintairov[1]

[1] Ioffe Institute,
194021 St. Petersburg, Russia
[2] St. Petersburg Electrotechnical University „LETI“,
197022 St. Petersburg, Russia
[3] St. Petersburg State University,
199034 St. Petersburg, Russia

E-mail: vdrodin@stud.etu.ru

Received May 5, 2025
Revised June 24, 2025
Accepted September 18, 2025

Using scanning probe microscopy, the relief and variations of the surface potential of MgF_2, SiN_x, SiO_2 dielectric coatings obtained by thermal evaporation, plasma-activated chemical deposition, and thermal oxidation of silicon, respectively, were studied. Compared with the first two, spatial fluctuations of the volume charge of the SiO_2 coating are minimal. This allowed us to accurately study the charge states of Au nanoparticles deposited on the SiO_2 coating and demonstrate the ability of scanning Kelvin probe microscopy to detect single-electron charge jumps on nanoparticles.

Keywords: Scanning Kelvin-probe microscopy, potential map, charge states detecting.

DOI: 10.61011/SC.2025.06.62054.8008

1. Introduction

There are currently a number of observations of effects that can be associated with the presence of fractional electron charge. They were discovered and studied in semiconductor systems with two-dimensional electrons in the fractional quantum Hall effect regime in a strong magnetic field [1,2] and in Wigner quantum dots in zero magnetic field [3]. In Wigner quantum dots, the fractional charge is formed due to the spontaneous generation of vortices of magnetic flux quanta by single-particle quantum electron states. The condition for the formation of such magneto-electron states is Wigner localization, which is possible in any system with two-dimensional electrons at a concentration below a critical level, which is met for most metals. Special interest in studying such states in metals is the registration of fractional charge of metallic nanoparticles, considered over 100 years ago by Ehrenhaft [4]. Ehrenhaft's experiment consisted of observing the movement of charged metallic nanoparticles in vacuum under the influence of an electric field, and the determination of the charge magnitude was based on a complex electrostatic calculation. In the present work, using the scanning Kelvin probe microscopy method (scanning Kelvin probe microscopy, SKPM), we implemented direct measurements of charge variations of metallic nanoparticles with sensitivity significantly better than the elementary charge. To do this, a special model structure was used, a flat capacitor based on silicon with micro-apertures in the upper metallic contact on an insulating gap made of SiO_2 in which the nanoparticles were located. The choice of substrate material was determined by the results of SKPM studies of charge distributions in it. Such studies, in addition, are interesting as a convenient direct diagnostics of the passivating properties of dielectric coatings. It is known that the use of dielectrics with embedded „corona“ charges is one of the basic methods of passivating semiconductor surfaces, in particular silicon solar cells, but the characterization of such coatings is more often done by indirect methods such as, for example, measuring the lifetime of nonequilibrium carriers [5,6].

The novelty of this study consists in the realization of the possibility to study thermal fluctuations of the potential of an isolated conductive particle, the single-electron dynamics of its potential using SKPM. In particular, jump-like changes in the potential of the particle were observed depending on time, when scanning the voltage on the capacitor, smoothly changing the charge on the surface of the micro-aperture with the particle by fractions of the elementary charge. Studies of charged states of nanoparticles by scanning probe microscopy methods are conducted quite actively [7–10]. The significant difference from our approach lies in the use of particles smaller in size by an order of magnitude, with Coulomb energy significantly higher than thermal energy. In addition, not single particles on an insulator of micron thickness are studied, but arrays of nanoparticles with a characteristic density of 10^3 particles per square micron^2, separated from the conductive substrate by a tunnel-transparent [7–9] layer of dielectric. Fluctuations of the potential of a conductive particle lying on a dielectric are determined not only by variations of the particle's own charge (intrinsic charge noise) but also by the behavior of external charges in the dielectric (induced charge noise).

In the absence of external charges, the particle with charge Q has a potential of $\sim Q/R$. External charges localized in traps in the dielectric far from the particle (at distances $\gg R$), create a far field E_1, in the region with the particle, which does not penetrate into the particle due to the induced charge dipole. The corresponding addition to the potential of the particle is $\sim E_1 R$. An external charge Q_2 on a single trap in the dielectric in immediate proximity to the particle creates a near field E_2. Shielding of this field inside the particle gives a contribution to the particle potential $\sim Q_2/R$.

To study, for example, the relationship between the amplitude of intrinsic charge noise and particle size, it is necessary to minimize induced charge noise. To reduce the contribution of external charges to the particle potential, a dielectric with a low trap density, i. e., a small volumetric charge and, consequently, E_1 is needed. If the traps are deep, with energy significantly greater than thermal, and the energy of charge capture on the particle itself, then the parasitic contribution from E_2 in the particle potential is also leveled.

The above explains the purpose of the work, namely: the optimization of a special model structure based on silicon substrates with micron dielectric coatings for detecting charge states and testing the possibilities of scanning probe microscopy to detect single-electron and sub-electron charge states in Au nanoparticles. Using the SKPM method, various dielectric coatings made by plasma-activated and thermal deposition methods, as well as thermal oxidation, were studied.

2. Experiment

Monocrystalline silicon plates (c-Si) of p-type with crystallographic orientation (100) were used as substrates. On the surface of clean c-Si plates, layers of dielectrics SiN_x, MgF_2, SiO_2 were formed, obtained by thermal evaporation (MgF_2), plasma-activated chemical deposition (SiN_x) and high-temperature oxidation in water vapor (SiO_2).

Plasma-activated pyrolysis installation (Rokappa) was used for depositing the SiN_x layer. Deposition was carried out at reduced pressure ($\sim 10^{-7}$ Topp) using high-frequency plasma. Reactive gases (monosilane, ammonia, helium) were supplied through filters to the upper part of the working chamber, where they decomposed under the influence of a discharge with power 50 W, excited by a resonator at ~ 13.5 MHz frequency. The plasma stimulation lowers the dielectric layer deposition temperature, accelerates dissociation of working gas molecules, generates radicals, intensifies particle diffusion to the substrate, their migration on the substrate surface, and promotes re-evaporation of adsorbed particles, increasing the rate of formation of nuclei, islands, and films overall. This method allows the formation of continuous SiN_x layers with thickness from 10 to 20 nm.

Thermal evaporation equipment VUP-5 was used for forming the MgF_2 layer. The MgF_2 charge was placed in a molybdenum crucible, and upon achieving vacuum in the chamber $\sim 10^{-6}$ Topp the crucible was heated by electric current to a temperature ensuring material evaporation. The thickness of the evaporated MgF_2 layer depends on the charge mass. The maximum uniform thickness reached 350 nm. Further thickness increase led to layer cracking due to overheating during evaporation.

Root mean square roughness of relief height rms (z) and surface potential rms (SP) for various dielectric coatings

Sample	SiN_x (0.2 μm)	SiO_2 (1.4 μm)	MgF_2 (0.5 μm)
rms(z), nm	3.0	0.3	1.3
rms(SP), mV	585	7	8

For SiO_2 layer formation on monocrystalline silicon (c-Si) an p-type plate with $\rho = 18\,\text{m}\Omega \cdot \text{cm}$ and crystallographic orientation (100) was used as the initial substrate. The plate was cut and underwent standard cleaning. A layer of SiO_2 with thickness $\delta = 1.4$ micrometers was grown by thermal oxidation in water vapor at temperature 1100 °C for 4 hours. Thickness data of silicon dioxide were obtained by spectral ellipsometry on a Semilab 2000 spectral ellipsometer.

SKPM measurements were carried out in normal and rarefied atmosphere (residual pressure $P \sim 10^{-2}$ Topp) in a vacuum chamber on the NT-MDT Integra Aura setup. Conductive contact cantilevers model CSG30 with moderate beam stiffness and sufficiently high-frequency resonance were used, which increased the sensitivity of SKPM surface potential (SP) measurements in dynamic modes of amplitude (AM) and phase (PM) modulation.

3. Results

3.1. SKPM measurements

Figure 1 shows the results of SKPM layer measurements. Surface morphology by height is presented in the top pictures, potential distribution — at the bottom; the table contains the results of mathematical processing of received data (root-mean-square surface roughness — rms).

The surface roughness of all layers does not exceed a few nanometers, except for individual defects, presumably microparticles of dust. It can be noted that the presence of such microparticles practically does not affect the potential distribution pattern. The surface of the MgF_2 layer has a granular structure and a relatively larger height spread (rms = 1.3 nm) compared to the SiO_2 layer (rms is only 0.3 nm). The greatest roughness is observed in the SiN_x layer, but here it does not exceed 3 nm.

In the potential distribution map, Figure 1, d of the SiN_x layer, several charged centers of different intensity can be observed. The difference in intensity can be caused both by the depth of the charged center and the magnitude of the charge. The potential drop across the surface

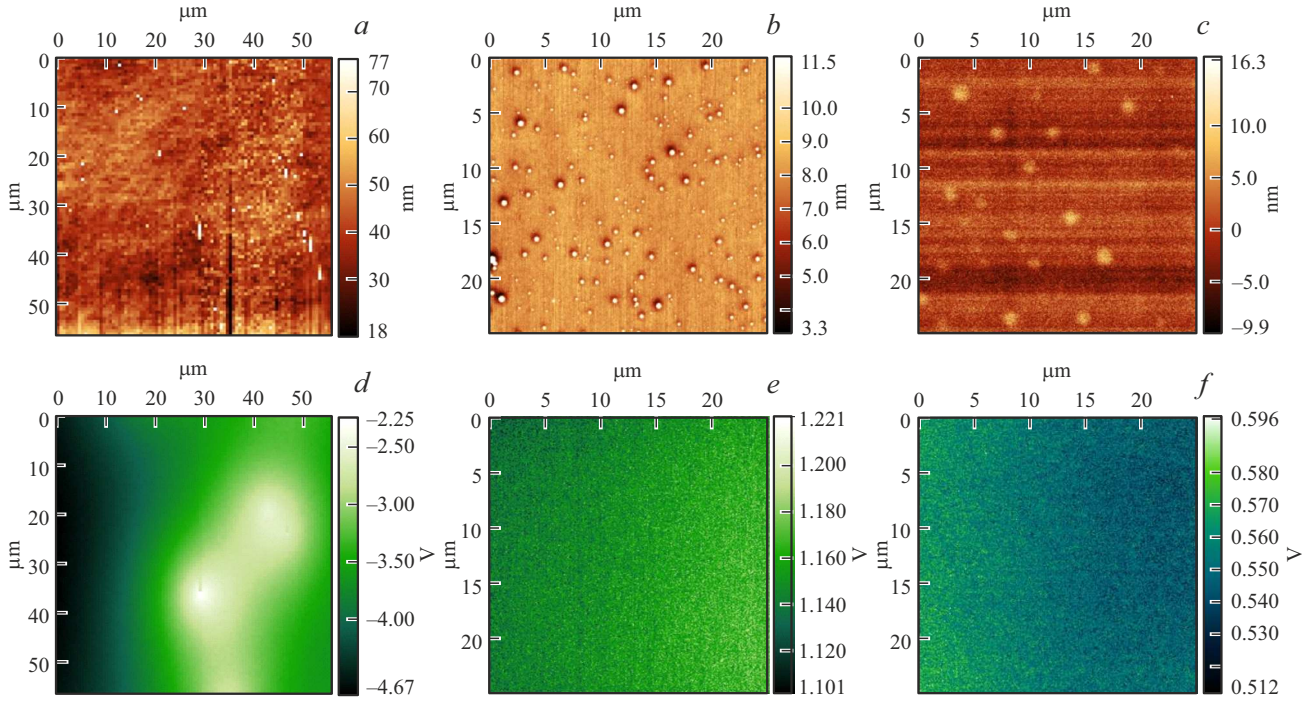

Figure 1. Results of SKPM measurements of dielectric coatings in normal atmosphere: top row — height profile, bottom — surface potential. *a, d* — layer SiN_x (0.2 μm); *b, e* — SiO_2 (1.4 μm); *c, f* — MgF_2 (0.35 μm).

exceeds 2 V. In layers obtained by the thermal method without the use of charged particles during the process, the potential distribution is uniform (Figure 1, *e, f*) and the potential drop is < 120 mV. Such smooth and insignificant potential changes, considering the 25-micron diagonal of the frame — horizontal field ~ 3 mV/μm — are observed on the surface of the thermal oxide in the absence of a conductive perforated contact on it. Basically, such a surface field can lead in the micron holes of our model structure to potential drops of units, a maximum of 10 mV, and on a 50-nanometer particle — to potential drops significantly less than 1 mV. The constant average slope in Figure 1, *e, f* does not change the noise amplitude since it is well known that surface roughness does not depend on its average slope. As a result, the root-mean-square deviations of the potential are 7–8 mV, comparable to the hardware noise of the measuring setup.

For further studies, layers of thermal oxide SiO_2were chosen, as they have minimal rms values both of roughness and potential, and, moreover, the method allows obtaining layers of any thickness without degrading quality.

3.2. Sensitivity of the SKPM method to charged states

Special model structures were created to study the sensitivity of the method. The overall topology is shown in the inset to Figure 2. The structure has a construction similar to a flat capacitor. The upper flat contact has holes with a diameter of $\sim 3\,\mu$m, into which it was possible to deposit single colloidal gold particles with a size of 40 nm. A voltage sweep ± 100 mV was applied between the upper and lower contacts, and during the voltage variation between the capacitor plates, one and the same 1 μm long line passing through the Au nanoparticle was scanned. This allowed monitoring the potential change both over the particle and at a distance from it.

Outside the particle over the dielectric surface, a gradual increase of the potential signal from 0.22 to 0.25 V is observed, caused by partial leakage of the capacitor field (see schematic in the inset of Figure 2) in the hole region with a diameter $D = 3.34\,\mu$m. Nonlinearity of signal growth can be associated with a slight drift of the signal over the dielectric, less than 0.03 mV/s in absolute value. The real potential change may be greater than the measured one due to instrumental contribution (discussion below). A change in voltage $\Delta V = 0.2$ V between the upper and lower contacts corresponds to a change in the total surface charge in the hole region of $\Delta q = 280e$ ($\Delta q = \varepsilon\varepsilon_0 \Delta V \pi D^2/\delta$). In the absence of the particle, the charge is distributed over the hole surface. Over the particle, upon capture of one or several of these electrons, the potential changes abruptly (Figure 2, line *1*). We associate such changes with thermal fluctuations of the particle potential. The characteristic height of the jumps is 10 mV or a multiple thereof (jumps marked by arrows), which corresponds in order of magnitude to the thermal energy (25 mV). The width of the jumps is also about 10 mV. Considering the voltage sweep speed on the lower contact of 0.5 mV/s, it is

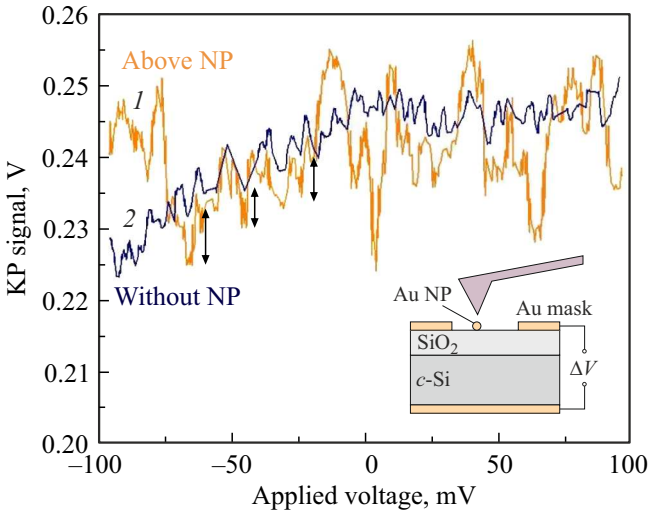

Figure 2. The signal values of the surface potential above the Au nanoparticle (line *1*) and above the dielectric surface (line *2*) during the application of the $\Delta V = 0.2$ V sweep voltage at a rate of 0.5 mV/s between the upper and lower contacts of the structure. The distance between the probe and the sample is 20 nm. The diagram of the special structure is shown in the inset.

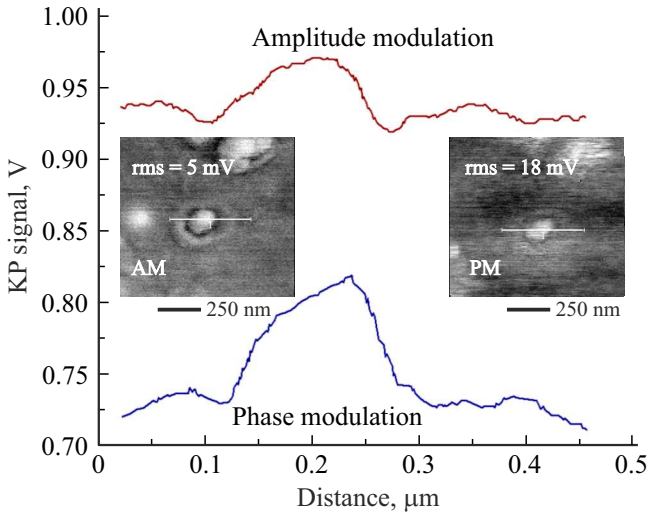

Figure 3. SKPM measurements of the potential over a 50-nanometer Au particle in a rarefied atmosphere. Signal profile over the particle in amplitude modulation mode (upper line) and phase modulation mode (lower line). Insets show the *SP* signal in AM and PM modes. In both modes, the distance between the probe and the sample is 20 nm.

obtained that approximately every 20 s the particle changes its charge by a jump.

Estimate the experimental signal by assuming the nanoparticle is spherical, i. e., its height equals its diameter ($2R = 40$ nm), and considering that the surface potential measurement is carried out at a height $h = 20$ nm from the surface. For an approximate analytical description of the particle potential, place an elementary charge in the center of the sphere. One electron, removed at a distance R from the dielectric (SiO_2, $\varepsilon = 4$), at a height $2R + h$ above the dielectric (i. e., at a height h above the top of the sphere) creates a potential [11]:

$$\varphi = \frac{e}{4\pi\varepsilon_0(R+h)} - \frac{e(\varepsilon-1)}{4\pi(\varepsilon+1)\varepsilon_0(3R+h)} \cong 25\,\text{mV}.$$

In the experiment, the characteristic oscillation amplitude,$\Delta SP = 10$ mV (AM SKPM data, AM — amplitude modulation), is 2.5 times less than this value.

Consider the instrumental contribution. Variations *SP* were measured in AM SKPM mode and therefore underestimate the real potential jumps. As seen in Figure 3, PM SKPM mode (phase modulation), having a signal-to-noise ratio worse by a factor of 2, more accurately determines *SP* signal jumps over submicron areas.

AM and PM images (see insets in Figure 3) differ both quantitatively and qualitatively (see the potential spot to the left of the particle on the AM image). Due to the large capacitive contribution of the cantilever and the probe side edges to the AM signal, its values may depend on the probe height above the surface. In the PM signal, the contribution of the capacitive interaction of the probe tip with the sample dominates. The PM image was measured after the AM image. The spot nature in the potential may also be caused by a random contact of the probe with the sample and local charge injection. The magnitude of the AM and PM signal jumps over the particle is not affected by the discussed qualitative image mismatch.

Taking into account the data of Figure 3, the real oscillation range over the particle in Figure 2 can be considered to be ~ 2 times larger, i. e., $\cong 20$ mV. As a result, the AM SKPM measured 10 mV *SP* signal oscillations (see Figure 2) correspond to single-electron charge jumps.

Thus, AM SKPM mode provides a better signal-to-noise ratio than the phase modulation mode. However, the measured potential jumps can underestimate the real jumps by at least a factor of 2. Taking into account the given calculation, this justifies considering the measured potential variations over an isolated gold particle as single-electron charge jumps, which is proof of very high method sensitivity for charge detection.

4. Conclusion

SKPM studies of thick dielectric coatings produced by various methods have been carried out. A significant dependence of the „roughness“ of the surface potential on the layer deposition technology is shown. Using an optimal dielectric silicon oxide layer of micron thickness with minimal surface potential fluctuations, a high sensitivity of the SKPM method is demonstrated, its ability to detect single-electron charged states of gold nanoparticles on such a layer.

Funding

The work was supported by the Russian Science Foundation grant No. 24-22-20014 and SPbNF grant 24-22-20014 (A.V. Ankudinov, V.D. Rodin, A.M. Mintairov). Work on gold particle deposition was supported by SPbU, project code 122040800254-4.

Conflict of interest

The authors declare that they have no conflict of interest.

References

[1] D.C. Tsui, H.L. Stormer, A.C. Gossard. Phys. Rev. Lett., **48**, 1559 (1982).
[2] J. Martin, S. Ilani, B. Verdene, J. Smet, V. Umansky, D. Mahalu, D. Schuh, G. Abstreiter, A. Yacoby. Science, **305**, 980 (2004).
[3] A.M. Mintairov, V.Yu. Axenov, D.V. Lebedev, A.S. Vlasov, A.S. Frolov, E.V. Ponamarev, V.S. Stolyarov. Phys. Rev. B, **111** (4), #0454102025 (2025).
[4] F. Ehrenhaft. Anzeiger Acad. Weiss (Vienna), **110**, 118 (1910).
[5] R.S. Bonilla, B. Hoex, P.R. Wilsham. Phys. Status Solidi A, **214** (7), 1700293 (2017).
[6] S.P. Muduli, P. Kale. Mater. Sci. Semicond. Process., **154**, 107202 (2023).
[7] A. Tekiel, Y. Miyahara, J.M. Topple, P. Grutter. ACS Nano, **7** (5), 4683 (2013).
[8] Y. Zhang, O. Pluchery, L. Caillard, A.-F. Lamic-Humblot, S. Casale, Y.J. Chabal, M. Salmeron. Nano Lett., **15**, 51 (2015).
[9] Y. Abbas, M. Rezeq, A. Nayfeh, I. Saadat. Appl. Phys. Lett., **119**, 162103 (2021).
[10] B. Chatelain, A.E. Barraj, C. Badie, L. Santinacci, C. Barth. New J. Phys., **23**, 123009 (2021).
[11] *General Course of Physics*. Ucheb. posobie dlya vuzov. V 5 t. T. 3. *Electricity*, Pod red. D.V. Sivukhin (M., Fizmatlit, 2004). (in Russian).

Translated by J.Savelyeva